# Uncertainty in Parameterized Convection Remains a Key Obstacle for Estimating Surface Fluxes of Carbon Dioxide

Andrew E. Schuh[1] and Andrew R. Jacobson[2,3]

[1]Cooperative Institute for Research in the Atmosphere (CIRA), Colorado State University, Fort Collins, CO USA
[2]CIRES, University of Colorado, Boulder, CO USA
[3]NOAA Global Monitoring Laboratory, Boulder, CO USA

**Correspondence:** Andrew Schuh, aschuh@atmos.colostate.edu

**Abstract.** The analysis of observed atmospheric trace gas mole fractions to infer surface sources and sinks of chemical species relies heavily on simulated atmospheric transport. The chemical transport models (CTMs) used in flux inversion models are commonly configured to reproduce the atmospheric transport of a general circulation model (GCM) as closely as possible. CTMs generally have the dual advantages of computational efficiency and improved tracer conservation compared to their parent GCMs, but they usually simplify the representations of important processes. This is especially the case for high-frequency vertical motions associated with diffusion and convection. Using common-flux experiments, we quantify the importance of parameterized vertical processes for explaining systematic differences in tracer transport between two commonly-used CTMs. We find that differences in modeled column average $CO_2$ are strongly correlated with the differences in the models' convection. The parameterization of diffusion is more important near the surface due to its role in representing PBL mixing. Accordingly, simulated near-surface *in situ* measurements are more strongly impacted by this process than are simulated total-column averages. Both diffusive and convective vertical mixing tend to ventilate the lower atmosphere, so near-surface measurements may only constrain the net vertical mixing and not the balance between these two processes. Remote sensing-based retrievals of total column $CO_2$, with their increased sensitivity to convection, may provide important new constraints on parameterized vertical motions.

## 1 Introduction

The analysis of atmospheric $CO_2$ mole fraction observations, including both *in situ* measurements and remote sensing retrievals of column average $CO_2$ ($XCO_2$), depends heavily on knowledge of atmospheric transport. This is the case for flux inversion models which use simulated atmospheric transport to interpret measured gradients of trace gas mole fractions to estimate surface fluxes of those species. Determining the magnitude, distribution, and causes of terrestrial and oceanic carbon sinks by interpreting $CO_2$ measurements in the context of modeled transport has a long history (Keeling et al., 1989a, b; Denning et al., 1999b; Gurney et al., 2002; Stephens et al., 2007). The recent work of Schuh et al. (2019) demonstrates that despite many years of progress in improving transport models, uncertainty and bias in simulated transport remains a key source of uncertainty in atmospheric inverse model results. In that work, the authors found a systematic dependence between optimized fluxes for large zonal regions and the corresponding transport model used in that system. That analysis found that in an ensemble of

state-of-the-art inversion models, the biggest systematic differences in optimized annual sources and sinks are in the latitudinal band from the equator to 45°N (Figure S1). The northern midlatitudes between 23° N and 67° N generate some of the biggest $CO_2$ signals in the atmosphere, due to the magnitude and seasonality of surface fluxes. Fossil fuel $CO_2$ emissions also are concentrated in this latitude band, with large emitters in North America, Europe, and Asia accounting for almost 80% of the 10 PgC/yr global fossil fuel emissions (Oda, 2018). The majority of the land and ocean net sink inferred from inversions is also concentrated in this zonal band. As a 2015-2018 mean, the OCO-2 v9 MIP inversion ensemble finds that this region accounts for between 75% and 80% (between 3.55 - 3.7 PgC/yr of the 4.63 PgC/yr total of the global land and ocean carbon sink (Peiro et al., 2021), depending on the use of either *in situ* (IS) constraints or land nadir plus land glint (LNLG) data. The terrestrial component of this mean sink is characterized by intense seasonal and diurnal variability, the signals of which are exported both polewards and equatorwards by advective and convective processes, which themselves are seasonally variable (D'Arrigo et al., 1987; Barnes et al., 2016). The tropical and high-latitudes signatures of midlatitude surface exchange depend strongly on the rate at which emissions signals are exported from the midlatitudes.

Key carbon cycle questions are subject to the uncertainty in the midlatitude export rate, the rate at which carbon is transported out of the atmospheric column over the midlatitudes, as simulated by chemical transport models (CTMs). A recurring question about the global carbon cycle is whether the long-term terrestrial carbon sink should be attributed to the tropics or to the midlatitudes (e.g. Schimel et al. (2014)). Terrestrial ecosystems around the world are all affected by changes in climate and atmospheric composition, but certain processes repeatedly emerge as potential explanations for increasing terrestrial sinks in tropical, mid-latitude and artic zones. For the northern midlatitudes, these theories include recovery from past land use practices and the impacts of nitrogen deposition (Norby and Zak, 2011; Craine et al., 2018; Penuelas et al., 2020). At higher latitudes, the expansion of boreal forests due to changing climate plays a role (Malhi et al., 1999), but the importance of that process is yet to be fully established. In the tropics, an area dominated by high gross primary production year-round, uncertainties dominate our understanding of the relative impacts of deforestation, climate forcing, and $CO_2$ fertilization (Lloyd and Farquhar, 2008; Norby and Zak, 2011). Uncertainties for fluxes inferred from inversions in these large zonal bands are still too large to make confident statements about mean annual $CO_2$ fluxes, their annual cycles, and therefore, their causes. Another topic of current interest touched upon by the midlatitude export rate is the changing seasonal cycle amplitude (SCA) of atmospheric $CO_2$ mole fractions at high latitudes (Graven et al., 2013; Liu et al., 2020). It is not clear the extent to which high-latitude carbon cycle processes are responsible for this observed growth in SCA, compared to the alternative possibility that this change is imported from midlatitudes.

Research funded by both OCO-2 and ACT-America has established that the rate at which $CO_2$ flux signals are exported from the midlatitudes varies strongly between two of the most commonly used CTMs, GEOS-Chem and TM5 (Schuh et al., 2019). This result was recently highlighted in Schuh et al. (2022) where the authors illustrated that the conclusions of a recent paper estimating the natural Chinese biospheric $CO_2$ sink (Wang et al., 2020) could be explained by differences among the CTMs being used in the atmospheric inversions considered.

In this paper, we look into the causes for the differences in transport between GEOS-Chem and TM5 and show, in particular, that parameterized vertical mixing plays a key role in how inverse models built on these CTMs estimate surface sources

and sinks of $CO_2$. It is important to note that in order to simulate parameterized vertical mixing in CTMs, particularly deep convection, it is necessary to reduce the complexity, and often the time-space resolution, of the parent GCM model output. For example, an algorithm which iteratively recovers multiple subgrid scale plume structures such as the Relaxed Arakawa Schubert scheme must often be summarized in a CTM by a single plume structure often running at 5-10 times coarser time and space resolutions. Significant information could be lost in these averaging processes and could potentially impose meaningful bias into estimates of vertical mixing. Even without such information loss, the GCMs producing some of the most commonly used reanalysis products in the world can differ dramatically in their estimates of convective activity. CTMs, particularly those used to advect long lived trace gases, must be able to simultaneously conserve tracer mass while attempting to faithfully reproduce transport from the GCM which produced the driving meteorology. This is particularly important when applied to convective mixing, as errors can often arise in parameterizations of this process, many of which were not designed with the intent to move long lived tracers.

In summary, this work attempts to establish the degree to which transport differences between GEOS-Chem and TM5 are associated with parameterized convection and diffusion in the two models.

## 2 Methods

### 2.1 Transport Models

The simulations for TM5 and GEOS-Chem were run from the start of 2000 through the end of 2018 and the methodology closely follows what was performed in Schuh et al. (2019) with minor updates to transport model version and common $CO_2$ fluxes.

#### 2.1.1 TM5/ERA-interim

TM5 is a global offline chemical transport model based on the predecessor model TM3 (Houweling et al., 1998; Dentener, 2003), with the capability of using two-way nested grids and including improvements in the advection scheme, vertical diffusion parameterization, and meteorological preprocessing of the wind fields (Krol et al., 2005). TM5 simulates advection, deep and shallow convection, and vertical diffusion in both the planetary boundary layer and free troposphere. For the analyses reported here, the model is driven by ECMWF ERA-interim (ERA-i) reanalysis meteorology, which is computed using a spectral formulation having 80 kilometers horizontal resolution. TM5 uses a 25 layer subset of ERA interim's 60 levels, extending to 0.01 hPa. Winds and mass fluxes from ERA-i are preprocessed by TM5 into coarse geographic grids, with attention to creating fields that conserve tracer and dry air mass. Like most numerical weather prediction models, advection in the parent ECMWF model is not strictly mass-conserving, so this preprocessing step is designed to enforce tracer mass conservation. This feature is considered crucial for long lived trace gas modeling. For simulations reported in this paper, TM5 was run at a global 3° longitude x 2° latitude resolution with a dynamically-variable time step with a maximum length of 90 minutes. This overall timestep is dynamically reduced to maintain numerical stability, generally during times of high wind speeds. Transport opera-

tors in nested grids are modeled at shorter timesteps, so processes at the finest scales are conducted at an effective timestep of one-quarter the overall timestep. We will use "TM5" to refer to this configuration of TM5 with ERA-i meteorology.

Version Cy31r2 of the Integrated Forecasting System (IFS) model was used to create the ERA-interim reanalysis (Dee et al., 2011) driving the present TM5 simulations. The IFS uses the Tiedtke convection scheme (Tiedtke, 1989), which provides upward and downward plume entrainment and detrainment mass fluxes at each model level. The IFS has continuously incorporated improvements to its convective parameterization, and major changes relevant to ERA-interim convection are detailed in Dee et al. (2011). These mass fluxes are combined into a convective mixing matrix representing mass transfer among all cells in a vertical column. The no-mass-flux boundary condition at the surface and convective top, along with a mass conservation constraint, determine the off-diagonal values of this mixing matrix. This permits nonlocal mixing among all levels with convective activity within a single mixing operation. For a complete description of this procedure in the TM3 model we refer readers to Heimann and Korner (2003).

In TM5, vertical diffusive fluxes are then added to the convective mixing matrix and the summed mixing matrix is applied to the tracer mass vector for a column of air. While vertical diffusion is imposed throughout the free troposphere, that mixing is much stronger within the diagnosed planetary boundary layer, following Holtslag and Moeng (1991) as described in Krol et al. (2005). Mixing from the surface is explicitly modeled as layer-to-layer diffusion, and as a result there are often strong vertical gradients in TM5 near the surface, for instance due to large northern midlatitude fossil fuel $CO_2$ emissions. In this scheme, convection and vertical diffusion are handled by a single step in the sequence of transport operators. To turn off convection or diffusion in TM5, we interceded in this vertical mixing operator and nullified the mixing due to one or the other process.

### 2.1.2 GEOS-Chem/MERRA2

GEOS-Chem (Bey et al., 2001; Lin and Rood, 1996) is an offline global chemical transport model developed by an extensive global community of researchers, including teams at Harvard University and the Global Modeling and Assimilation Office (GMAO) at NASA's Goddard Space Flight Center (GSFC). GEOS-Chem separately simulates advection, deep and shallow convection, and vertical diffusion in the planetary boundary layer. We use the version 12.0.2 of GEOS-Chem which has improved tracer advection, and smoother local tracer gradients in time and space, over previous versions (Lee and Weidner, 2016) due to transporting tracers with dry air mass as opposed to wet air mass. Meteorology to drive the GEOS-Chem simulations is regridded from MERRA2 reanalyses (Rienecker et al., 2011; Bosilovich, 2015) to 2.5° longitude x 2° latitude. GEOS-Chem is run using a 15 minute dynamical timestep. The native 72 levels of the MERRA2 grid are reduced to 47 levels for use in GEOS-Chem by aggregating levels above approximately 70hPa. This configuration of GEOS-Chem with MERRA2 meteorology is abbreviated "GEOS-Chem" in the following text.

Parameterized vertical motion in GEOS-Chem is composed of (1) moist convective processes and (2) planetary boundary layer (PBL) mixing. The Relaxed Arakawa–Schubert (RAS) scheme of Moorthi and Suarez (1992) is used within the parent Goddard Earth Observing System (GEOS) model used to create MERRA2. In particular, GEOS-5 uses an updraft-only detraining plume cloud model, which results in the two relevant output variables for GEOS-Chem convection: cloud upward moist convective mass flux and detrainment cloud mass flux. Convective transport in GEOS-Chem is then simulated with a

single-plume scheme using the archived three hourly updraft and detrainment convective mass fluxes (Wu et al., 2007). It is worth noting that GEOS-Chem reproduces the three hourly average convective transport in the GEOS-5 GCM but any interaction of transport and tracers on finer temporal scales is lost. Furthermore, whenever convection is found within a gridcell, the GEOS-Chem convection code triggers a complete mixing in the atmospheric column beneath the lowest level with convection. Because of this, diffusive mixing cannot be logically separated from convection in GEOS-Chem, especially in regions characterized by persistent convection.

The implementation of convective mixing in GEOS-Chem is intended to represent the single-updraft convection scheme from its parent GEOS-5 model. The details of how this is done are described in Stanevich (2018). Among significant characteristics are the use of a timestep, a sub-timestep of the GEOS-Chem transport timestep, specifically for convective processes, and a sequential mixing algorithm. There is some question about the impacts of space- and time-averaging of parent-model convective mass flux and vertical velocity fields on GEOS-Chem convection. These issues were explored by Yu et al. (2017), who found that there are significant differences in GEOS-Chem transport as the resolution of the driving meteorology is varied.

Two options in GEOS-Chem exist for PBL mixing, (1) a non-local scheme based upon Holtslag and Boville (1993) adapted for GEOS-Chem by Lin and McElroy (2010), and (2) a simple "well mixed" scheme in which PBL tracers are mixed evenly from the surface to the top of the PBL as diagnosed by GEOS. In this work, we use the "well mixed" scheme in the PBL. Both the convection and PBL mixing can be turned on or off using standard configuration options.

### 2.2 $CO_2$ simulations

We conduct $CO_2$ forward runs in both models from January 1, 2000 through December 31, 2018, similar to those in Schuh et al. (2019) but with updated CarbonTracker fluxes. Initial $CO_2$ concentrations and surface fluxes throughout the simulation come from the CarbonTracker CT2017 release (Peters et al., 2007, with updates documented at http://carbontracker.noaa.gov) for the period January 1, 2000 to December 31, 2016 and then CT-NRT.v2019-2 for January 1, 2017 to December 31, 2018. The initial condition field used by both models at January 1, 2000 was created by averaging together 15 years of $CO_2$ mole fraction fields from CT2016, each sampled on January 1st of the years 2001-2015 and then scaled to the year 2000. The scaling was performed by sampling the marine boundary layer from these mole fraction fields and then comparing them to the NOAA marine boundary layer reference surface (https://www.gml.noaa.gov/ccgg/mbl) for the target date. For use in GEOS-Chem, the CarbonTracker initial condition was interpolated vertically in pressure and horizontally in space to the GEOS-Chem grid as described in Schuh et al. (2019).

CT2017 and CT-NRT.v2019-2 $CO_2$ optimized fluxes are partitioned into four flux terms: the imposed fossil fuel term, the optimized biological flux, the imposed fire emissions flux, and the optimized oceanic flux. Each of these terms is tracked independently as a tagged tracer, along with a background tracer representing the initial condition. As a result of the optimization procedure, these fluxes are generally consistent with observed atmospheric $CO_2$ mole fractions. They were created with an inverse modeling system based on TM5 and may have artifacts and inaccuracies associated with that model's atmospheric transport and with assumptions used in the CarbonTracker data assimilation system. However, in the analyses conducted here we do not require that these fluxes be completely correct, only that they are reasonably representative of actual atmospheric

$CO_2$ exchange with the surface. While there is certainly large uncertainty in CT2017 fluxes, important aspects of the flux signals, such as seasonal terrestrial net ecosystem exchange in northern latitudes, placement of fossil fuel emissions, and estimates of biomass burning are generally consistent with the results from other inversion systems that assimilate surface *in situ* $CO_2$ data (Peylin et al., 2013). We found a small non-conservation of tracer mass in GEOS-Chem, with a monotonic loss of about 0.25% in fossil fuel $CO_2$ over the period 2000-2018. Non-conservation of natural fluxes was about half as small. The global mass differences for these tracers were removed from the concentration data before analysis.

### 2.3 Vertical Mixing Perturbation Simulations

We ran three perturbation experiments on each transport model, with each simulation extending from Jan 1, 2016 to Dec 31, 2018. Control runs use the standard vertical transport in the models, unmodified from their stock configurations. The first experiment involved turning off convection in both CTMs. These will be called the "no convection" or "NC" runs. The second experiment involved leaving convection on but turning off diffusive mixing in the models. These will be termed "no diffusion" ("ND") runs. It should be noted that vertical advection as part of the resolved wind fields in each model still remains in both perturbation and control runs for both models. We introduce the notion of a "convective effect", which we are defining as control - NC and a "diffusive effect" as control - ND. The diffusive and convective transport effects are not independent. The two processes have significant interactions such that total parameterized vertical transport is greater than the sum of the convective and diffusive effects. Exploring this nonlinear interaction, while intriguing, is beyond the scope of this paper. As a result, experiments in which both convection and diffusion are turned off will not be discussed.

## 3 Results

In this section, we show the differences between the TM5 and GEOS-Chem control simulations, and differences in the NC and ND cases from several perspectives. First, we show a zonally averaged vertical "curtain" by latitude which illustrates how the differences manifest themselves in the vertical. We then show two projections of the differences relevant to the major types of observational data used in flux inversions of $CO_2$. The first is time-latitude (Hovmöller) plots of zonal-mean column-average $CO_2$ ($XCO_2$), which is relevant to analysis of satellite $CO_2$ retrievals. The second is seasonal maps of differences in the planetary boundary layer at 400 meters above ground level, meant to represent transport impacts on the ground-based *in situ* observational network.

### 3.1 Vertical curtains

Zonal average "curtains" (latitude by vertical dimension) of $CO_2$ from the control and NC simulations in the two models are in presented in Figure 1. These curtains are shown for typical northern-hemisphere winter (February) and summer (August) conditions. The expected buildup of $CO_2$ from fossil emissions and terrestrial biospheric respiration in boreal winter is evident in the northern mid to high latitudes in both models' control simulations (panels a and b). The overall differences between the GEOS-Chem and TM5 control runs are shown in panel (c). The convective effects in the two models for February, and

the GEOS-Chem minus TM5 difference in convective effect, are portrayed in the second row, panels d-f. The difference in convective effects (panel f and l) bears a remarkable similarity to the control simulation difference (panel c and i).This suggests visually that the GEOS-Chem minus TM5 difference in zonal-mean $CO_2$ is strongly driven by the convective effect. Indeed the fields in are strongly correlated (February: panels a and c, r=0.72, $p < 0.0001$; August: panels d and f, r=0.83, $p < 0.0001$). This will be further discussed in section 4 below. The diffusive effect (not shown here) is about three times larger in magnitude, but is strongly concentrated near the surface. The diffusive effects are shown in Figures S2 and S3.

The last two rows of Figure 1 show the same quantities as the first two, but for northern hemisphere summer (August). Terrestrial biosphere uptake results in a deficit of $CO_2$ in the troposphere poleward of the northern midlatitudes. Again the difference in convective effect (panel l) is visually similar to the control simulation differences (panel i).

### 3.2 $XCO_2$ differences

Zonal averages of the GEOS-Chem minus TM5 difference in $XCO_2$ as a function of latitude and time are shown in the middle two columns of Figure 2. Three-year averages of the differences are shown in side panels and present a possible proxy or metric for the transport error effect on annual source/sink estimates of $CO_2$ from inversions. As in the previous vertical curtain plots, the convective effect differences shown in the middle row of Figure 2 bear a strong resemblance to total difference between the control runs shown in the top row of Figure 2. Vertical diffusivity effects as a column average (bottom row of Figure 2) are of a much smaller magnitude. It is also worth pointing out that despite the strong seasonal patterns of differences seen in total $CO_2$ (panel c and g of Figure 2), the annual mean differences in total $CO_2$ (panel d and h of Figure 2) and fossil $CO_2$ (panel a and e of Figure 2) are quite similar and thus likely driven by differences arising from fossil fuels.

Figure 3 shows the 2016-2018 spatially-resolved time mean $XCO_2$ difference between GEOS-Chem and TM5. This figure illustrates the zonal variability of the $XCO_2$ differences, which was not shown in Figures 1 and 2. The large band of negative differences evidenced by the blue band in the lower northern latitudes is driven in large part by differences aloft, shown in Figure 1, and not from differences near the surface. There is an anomalously high difference over China, which is not due to a deviation of the difference pattern aloft but by a combination of weaker mixing in GEOS-Chem and anomalously strong fossil fuel emissions over Eastern China. Reproducing panel c of Figure 1 only over the area of enhancement in Figure 3, approximately 105°E to 120°E longitude results in PBL concentrations that are enhanced by 1-2 ppm $CO_2$ over the majority of the lower 20-25 % of the atmosphere and is the strongest contributor to the column average results in the spatial anomaly seen in Figure 3.

Seasonal summaries of the $XCO_2$ (Figure 2) subsetted into 45 degree latitude bands are shown in Figure S4. There is excellent agreement between the differences in convective effect and the differences in the control simulations, suggesting that convection differences between GEOS-Chem and TM5 are the predominant control on seasonal $XCO_2$ transport differences.

### 3.3 Impacts on near-surface $CO_2$

In the planetary boundary layer near intense surface sources and sinks of $CO_2$, the monthly average differences in diffusive effect between the models are on the order of 10 ppm (Figure 4). This is an order of magnitude larger than the model differences

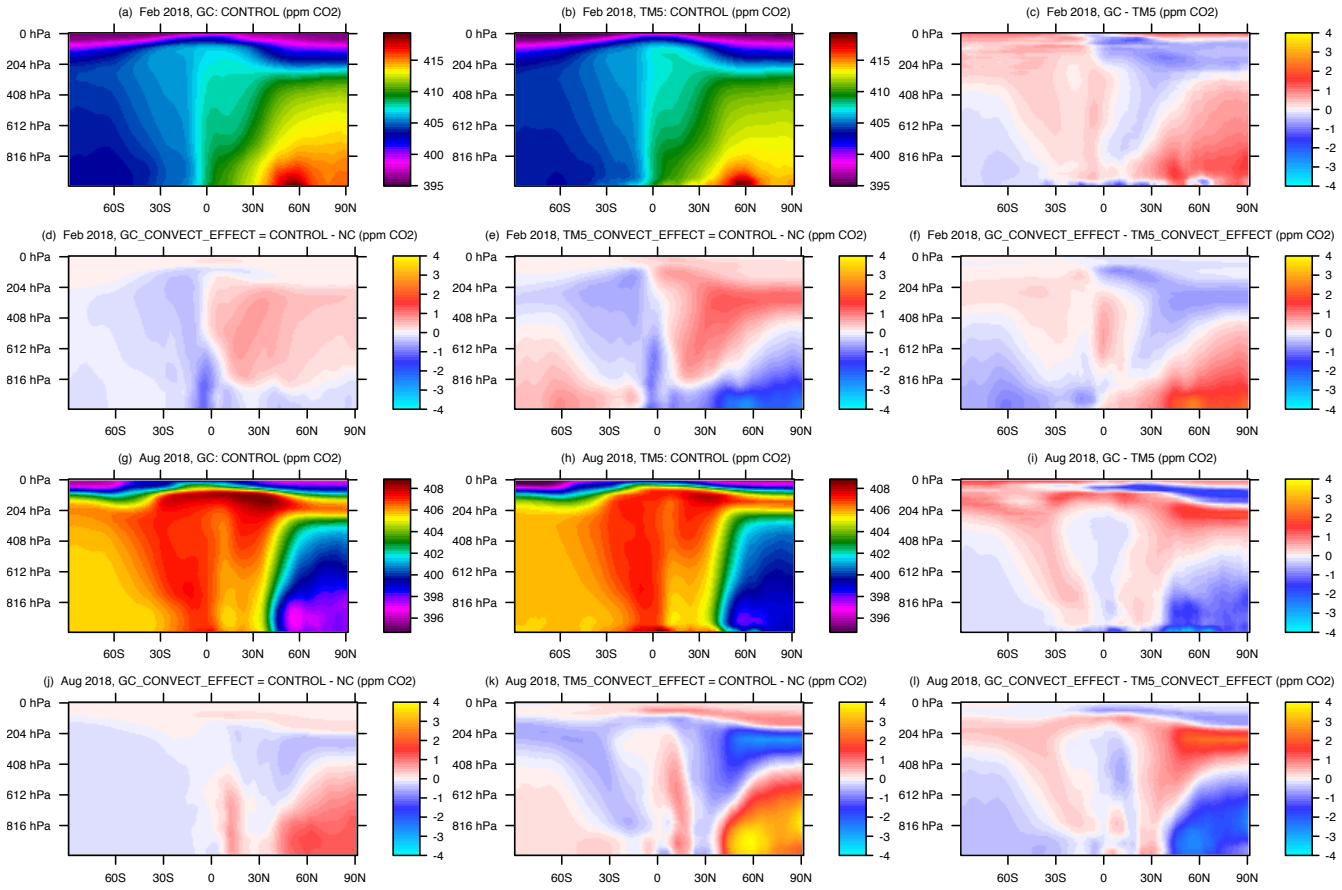


**Figure 1.** Vertical curtains of zonal-mean $CO_2$ dry-air mole fraction for February (top two rows) and August 2018 (bottom two rows). All quantities are monthly averages. The first and third rows (panels a-c and g-i respectively) show model control simulations and differences, averaged zonally. The second and fourth rows (panels d-f and j-l respectively) show the convective effect (control experiment minus the no convection, NC, experiment) in each model and the GEOS-Chem minus TM5 difference between them. The first column represents GEOS-Chem simulations, the second is TM5, and the third column is the GEOS-Chem minus TM5 difference.

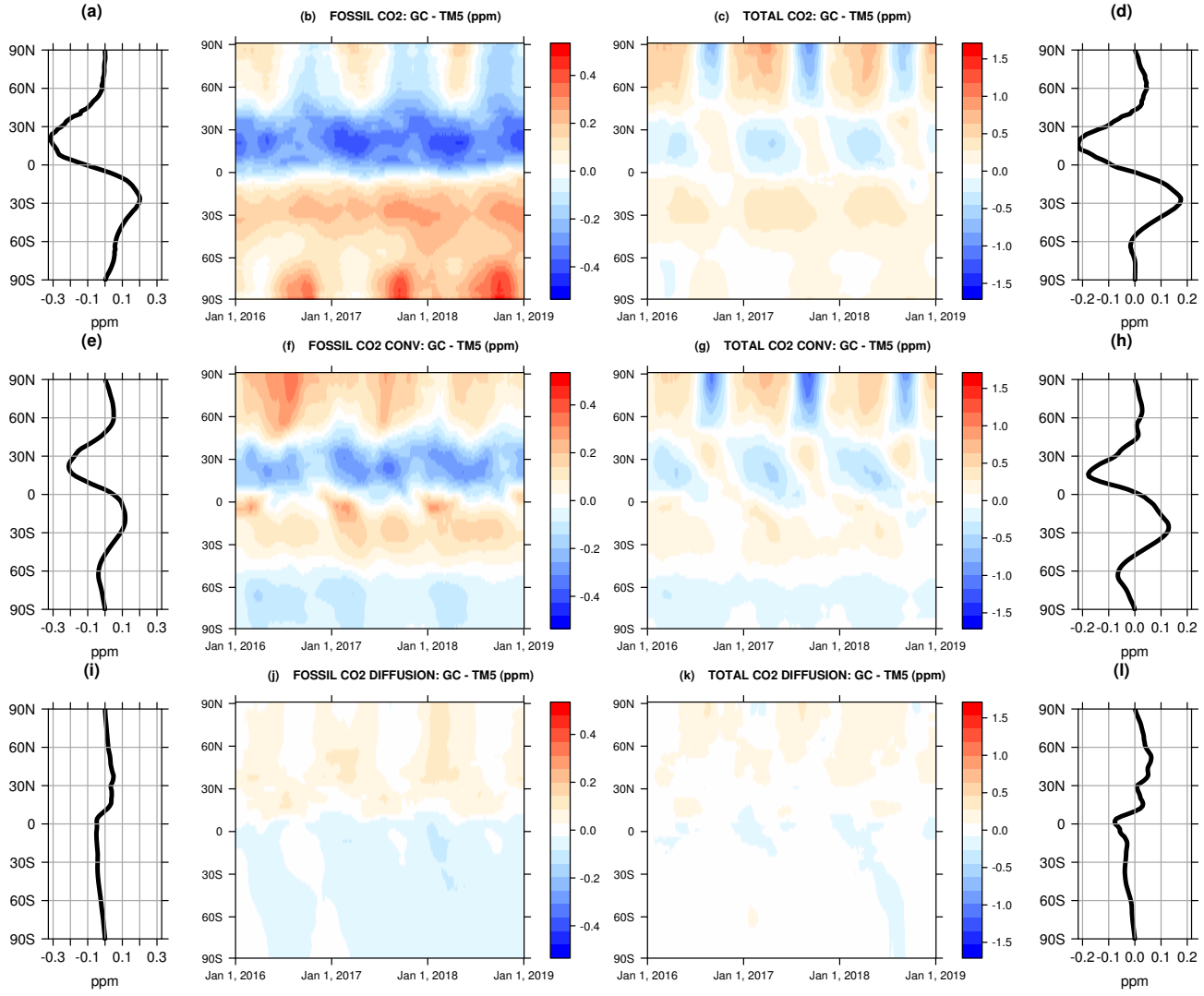


**Figure 2.** Zonally-averaged pressure-weighted average $CO_2$ differences between GEOS-Chem and TM5, plotted as function of latitude in side integrals and as a function of latitude and time in central panels, in dry-air mole fraction. Column 1 represents 3 year average of 2nd columns. Column 4 represents 3 year average of 3rd columns. Note the differences in scale between the fossil and total $CO_2$ plots.

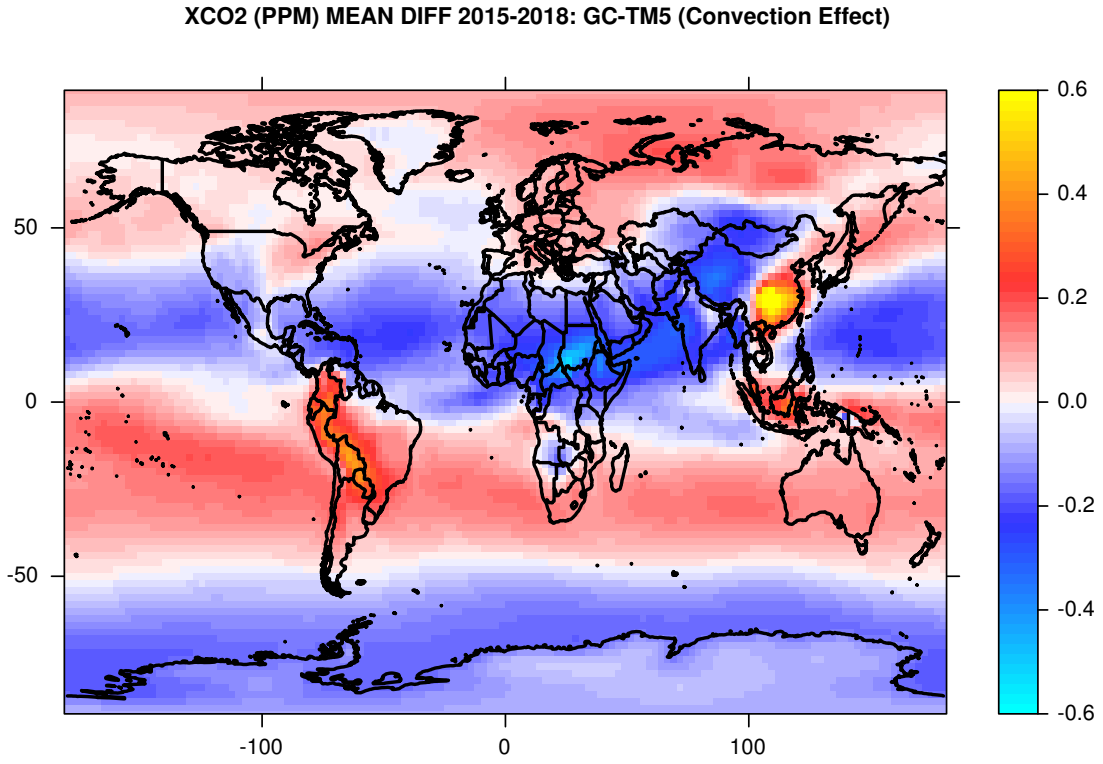


**Figure 3.** The 2016-2018 average $XCO_2$ difference between GEOS-Chem and TM5 "convective effects" (i.e. control - NC cases) using the TOTAL $CO_2$ tracer.

in the column seen in Figure 2. There is a marked seasonality to the difference of $CO_2$ mole fraction at this level (leftmost column, panels a,d, and g), and the convective and diffusive effect patterns in both seasons (topmost two rows, panels a-f) appear anti-correlated at large scales. We will return to discuss this in Section 4

## 4 Discussion

### Annual flux biases from convection uncertainty at zonal scales

Exploratory analysis on the location of long term carbon sinks is commonly performed by considering large zonal bands in order to contrast the tropics, extra-tropics and high latitudes (Stephens et al., 2007; Schimel et al., 2014), each of which has different mechanistic reasons to develop sources or sinks of carbon in a warming climate. The difference in convection effect across CTMs, as seen in right hand column of Figure 2, generates a significant first-order bias on these important annual-zonal scales.

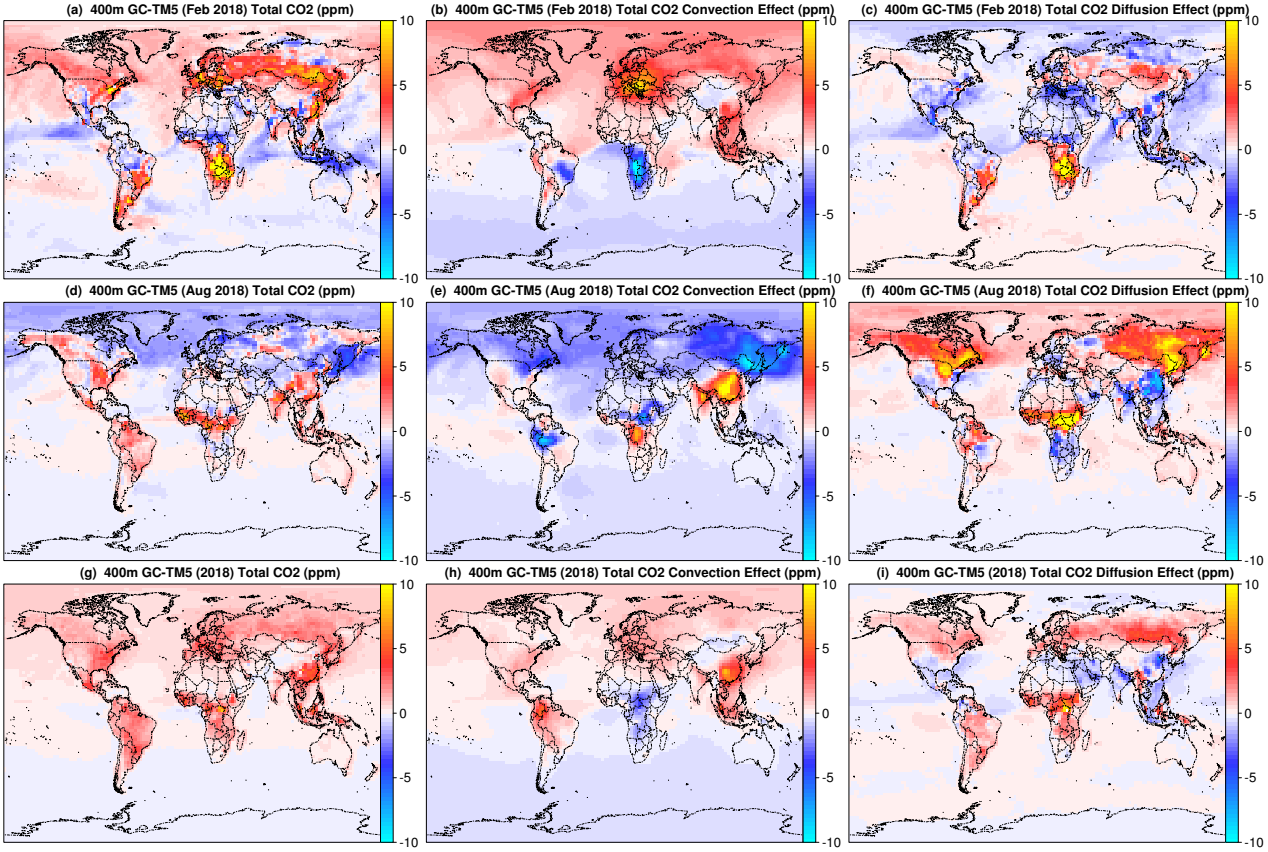


**Figure 4.** Monthly and annual average near surface model $CO_2$ differences. Results have been interpolated to the 2°x 2.5° GEOS-Chem grid and 400 meter height above ground level.

### Remaining model $XCO_2$ differences after accounting for convection

An examination of panels (c) and panel (f) of Figure 1 shows that while the convective effect difference largely explains the control simulation differences between the two models away from the surface, it does not extend to the same altitude as the control simulation differences. This remaining difference bears some similarity to the difference in ND runs (Figures S2 and S3), indicating that while convection may be the main driver of the vertical differences in the model, it is likely that low level PBL diffusivity differences also play a role.

### Seasonal Cycle of $XCO_2$

Agreement on the seasonal cycle of $XCO_2$ appears quite good between the GEOS-Chem and TM5 control runs, with the amplitude of the average zonal seasonal differences on the order of 1 ppm or less at 45°N and poleward. GEOS-Chem minus TM5 differences in modeled seasonal cycles at TCCON locations are 10-15% of the amplitudes reported by Lindqvist et al.

(2015). While this difference is small, it is likely still significant to science hypotheses attempting to explain observed decadal scale changes in seasonal amplitude (Graven et al., 2013). Accounting for differences in convection reduces that difference by another order of magnitude, resulting in great agreement in $XCO_2$ on seasonal cycle amplitude. Hence a focus on improving the modeling of convective mixing of trace gases could have a significant impact on the ability to constrain high-latitude seasonality.

**Regional Effects of Convection Uncertainty**

The effect of uncertainty in the parameterized modeling of vertical mixing, and convection in particular, drives systematic differences in $XCO_2$. These concentration differences then manifest themselves as the first order source of flux bias across large zonal bands amongst satellite $CO_2$ constrained flux inversion models (Schuh et al., 2019). However, in some regions there are notable exceptions to the zonal mean of transport differences. One of these is over eastern Asia in the general area of China (Figure 3). This anomaly to the zonal average largely arises from model differences in the spatially-varying convection field (Taszarek et al., 2021) acting on large regional sources of $CO_2$ fossil fuel consumption (Schuh et al., 2022). While total $CO_2$ is plotted in Figure 3, one can see that the signal comes largely from the fossil fuel related portion of the $CO_2$ budget (cf. Figures S5, S6 and S7). Similar patterns emerge across areas of critical biological importance, such as the Amazon and equatorial Africa (Figure S7) and even emerge at the national scales there (Figure S8). These could result in regional flux anomalies that are dependent on the particular CTM being used in a flux inversion.

**Compensating effects of turbulent mixing and deep convection in PBL**

While parameterized diffusion and convection cause mixing in different parts of the column, they both act to move signals of surface exchange up, away from the PBL and into the free troposphere. Historically, measurements of active and passive chemical species have been made more commonly within the PBL or at the surface than in the free troposphere. The availability of measurements near the surface without a correspondingly strong constraint on upper atmospheric abundances means that those measurements speak strongly to the overall rate of ventilation of the PBL, and not necessarily which process is responsible for the needed mixing. We speculate that CTMs may meet this constraint using a different overall balance of convection and diffusion. The combination of remotely-sensed total column abundance with *in situ* measurements concentrated in the PBL may help to provide the needed constraint on vertical distribution to identify a correct balance of these mixing processes. In particular, this is an area where aircraft observations, both campaign data (e.g. Atmospheric Tomography Mission (ATOM), Atmospheric Carbon and Transport – America (ACT-America) and more operational data (e.g. In-Service Aircraft for a Global Observing System (IAGOS), NOAA light aircraft profiles) could provide useful constraint.

**Potential Issues with Direct Comparison of GEOS-Chem and TM5 convection implementations**

The parent models for GEOS-Chem and TM5 simulate convection differently. Some of the vertical movement associated with convection is explicitly resolved, depending on the model grid resolution. Non-resolved movement is parameterized using

significantly different schemes. NASA's GEOS-5 MERRA2 reanalysis uses the Relaxed Arakawa-Schubert convection scheme (Moorthi and Suarez, 1992), an updraft-only detraining plume cloud model (Molod et al., 2012), to provide driving convective mass fluxes used for GEOS-Chem. Version Cy31r2 of the Integrated Forecasting System (IFS) model was used to create the ERA-interim reanalysis (Dee et al., 2011) used to drive the present TM5 simulations. The IFS uses the Tiedtke convection scheme (Tiedtke, 1989) to provide upward and downward plume entrainment and detrainment mass fluxes at each model level and as a means to represent shallow, intermediate, and deep convection. Both GEOS-Chem (Stanevich, 2018) and TM5 (based on the TM3 model from Heimann and Korner (2003)) interpret convective mass fluxes from their parent models to drive relatively simple mixing schemes. This mixing can be represented by a matrix specifying exchange among the layers in the column of a given grid cell.

While the RAS and Tiedtke convective parameterizations are different, we can still perform qualitative comparisons of the upward convective mass fluxes from the parent models under investigation here. While the downdraft component from TM5 is important, it is an order of magnitude weaker than the updraft component as can be seen in Figure S9. The comparison (Figure S9) shows convective activity that is significantly different between the two models and highlights shallow convection features driving lower tropospheric mixing in TM5 that do not appear in GEOS-Chem. This would appear to support past research highlighting differences between shallow convection features in MERRA and ERA-Interim (Posselt et al., 2012; Naud et al., 2014). This would suggest that the differences in CTM convective transport reported here result largely from differences in convection in the parent models as opposed to variations in how convective mixing is implemented in the CTMs. This confirms the findings of Folkins et al. (2006), Donner et al. (2007) and Orbe et al. (2017). Comparisons to long lived trace gases like $SF_6$ might allow more definitive conclusions about how differences in parent model convection, and differences in their re-implementations in CTMs, drive the large-scale differences seen in this paper Denning et al. (1999a); Peters et al. (2004). Other metrics such as the stratospheric age of air **?** could provide insight into the differences seen here.

**Looking forward**

Recent analyses suggest that vertical transport in GEOS-Chem may be responsible for systematic biases in model performance against comparisons to $CH_4$ and $SF_6$ observations (Schuh et al., 2019; Stanevich et al., 2021). Part of this suspected vertical mixing issue may be due to imperfect reproduction of parent GEOS5 model transport (Yu et al., 2017). In preliminary analysis of meridional gradients of trace gases, the GEOS5 parent model does not appear to exhibit the same systematic biases as the GEOS-Chem CTM (personal communication: Brad Weir, NASA-GMAO). When using offline parent convective mass flux fields, in theory, convective mixing of trace gases via resolved vertical velocity should be damped with increased averaging in time and space, and decreased horizontal model resolution (Yu et al., 2017). Furthermore, the coarse temporal nature, e.g. 3 hours or more, of the convective mass flux averaging leads to an information loss because the higher time resolution covariance between tracer fields and vertical motion is lost. The resolved vertical velocity in 0.5° by 0.667° MERRA2 is similar in location and magnitude to that from the approximately 80km ERA-interim (personal communication: Sourish Basu, NASA-GMAO). This should not be surprising due to the similar horizontal resolutions of the model fields and suggests that the averaging of

resolved vertical velocity fields to the coarser resolution CTM grids is likely not the reason for the differences shown in this paper.

Ideally, one would desire a CTM's transport to asymptotically converge to the parent model's transport as model spatial and temporal resolution increases to the native resolution of the parent model, but this has not been demonstrated. It is worth noting that past work (Prather et al., 2008) utilizing two CTMs acting on the same parent meteorology has demonstrated the difficulty in characterizing this convergence. Tests are currently under way with high time- and space-resolution GEOS5 meteorology via the GEOS-Chem High Performance (Martin et al., 2022) model to gauge this convergence. These tests will help to determine whether results such as Yu et al. (2017) are sufficient to explain all deficiencies in CTM vertical transport.

It is also worth noting that despite the clear patterns of difference in the large-scale convective mass fluxes from parent models used as inputs into GEOS-Chem and TM5 (see Figure S9), there are likely other factors at play which could cause differences in vertical transport. For its advection scheme, TM5 uses parent model mass fluxes and a corresponding flux form advection scheme, whereas GEOS-Chem explicitly uses interpolated parent model winds to diagnose mass fluxes for advection. The use of winds to drive advection, as opposed to mass fluxes, has been shown to be a likely source of errors and bias (Jöckel et al., 2001). As a result of this, tests are also currently underway using the GEOS-Chem High Performance (Martin et al., 2022) model to investigate the magnitude of this bias and to what degree those model errors, and related errors in horizontal divergence, might be related to vertical transport in GEOS-Chem (personal communication, Sebastian Eastham).

## 5 Conclusions

The systematic large-scale patterns in $XCO_2$ differences associated with transport first presented in Schuh et al. (2019) have been shown to result primarily from differences in the parameterization of convective mixing. This is the most important source of transport uncertainty for satellite-based flux inversion studies and of the same order as the expected biases in $XCO_2$ retrievals. We have shown that for the simulation of concentrations near the surface, diffusive mixing in the PBL has a bigger effect than deep convection. It can therefore be expected that inversions based upon *in situ* measurements would be more sensitive to modeled vertical diffusion in the PBL than modeled deep convection.

The significance of uncertainty in simulated convection for model ensembles assimilating $XCO_2$, such as those of Crowell et al. (2019) and Peiro et al. (2021), warrants further exploration of model convective parameterizations. Convection alone drives 10-15% differences in $XCO_2$ seasonality between the two models studied here, and explains the vast majority of total model differences in simulated $XCO_2$ seasonality. We also have shown that convection drives the majority of the meridional difference in annual average $XCO_2$, a proxy for the meridional distribution of annual source and sinks in the related flux inversion models. Therefore, we feel that future efforts to characterize transport uncertainty and how it relates to flux inversion results would benefit tremendously from a more thorough exploration of differences in parent model convection.

*Author contributions.* Author contributions as follows: A. S. and A. J. wrote the manuscript. A. S. performed the GEOS-Chem $CO_2$ simulations and performed analysis of results. A. J. was responsible for producing CT2017 and CT-NRT.v2019-2, and for running the perturbation simulations with TM5.

*Competing interests.* None.

*Disclaimer.* None.

*Acknowledgements.* Funding for work came from NASA via funded proposals of A. S. and A. J. Specifically, OCO-2 Science Team project (grant NNX15AG93G to Colorado State University and NNX12AP91G to the University of Colorado) and the Atmospheric Carbon and Transport (ACT)-America project, a NASA Earth Venture Suborbital 2 project funded by NASA's Earth Science Division (NNX15AJ07G to Colorado State University, and NNX15AJ06G to the University of Colorado). Results, analysis, and current publications related to the underlying v9 MIP atmospheric inversion models are available at their website (https://www.esrl.noaa.gov/gmd/ccgg/OCO2_v9mip/)

## References


Barnes, E. A., Parazoo, N., Orbe, C., and Denning, A. S.: Isentropic transport and the seasonal cycle amplitude of CO2, Journal of Geophysical Research: Atmospheres, 121, 8106–8124, https://doi.org/doi:10.1002/2016JD025109, 2016.

Bey, I., Jacob, D. J., Yantosca, R. M., Logan, J. A., Field, B. D., Fiore, A. M., Li, Q., Liu, H. Y., Mickley, L. J., and Schultz, M. G.: Global modeling of tropospheric chemistry with assimilated meteorology: Model description and evaluation, Journal of Geophysical Research: Atmospheres, 106, 23 073–23 095, https://doi.org/10.1029/2001JD000807, 2001.

Bosilovich, M. G.: Technical Report Series on Global Modeling and Data Assimilation, Volume 43 MERRA-2: Initial Evaluation of the Climate, Tech. rep., NASA-GMAO, https://gmao.gsfc.nasa.gov/pubs/docs/Bosilovich803.pdf, 2015.

Craine, J. M., Elmore, A. J., Wang, L., Aranibar, J., Bauters, M., Boeckx, P., Crowley, B. E., Dawes, M. A., Delzon, S., Fajardo, A., Fang, Y., Fujiyoshi, L., Gray, A., Guerrieri, R., Gundale, M. J., Hawke, D. J., Hietz, P., Jonard, M., Kearsley, E., Kenzo, T., Makarov, M., Marañón-Jiménez, S., McGlynn, T. P., McNeil, B. E., Mosher, S. G., Nelson, D. M., Peri, P. L., Roggy, J. C., Sanders-DeMott, R., Song, M., Szpak, P., Templer, P. H., der Colff, D. V., Werner, C., Xu, X., Yang, Y., Yu, G., and Zmudczyńska-Skarbek, K.: Isotopic evidence for oligotrophication of terrestrial ecosystems, 2, 1735–1744, https://doi.org/https://doi.org/10.1038/s41559-018-0694-0, 2018.

Crowell, S., Baker, D., Schuh, A., Basu, S., Jacobson, A. R., Chevallier, F., Liu, J., Deng, F., Feng, L., Chatterjee, A., Crisp, D., Eldering, A., Jones, D. B., McKain, K., Miller, J., Nassar, R., Oda, T., O'Dell, C., Palmer, P. I., Schimel, D., Stephens, B., and Sweeney, C.: The 2015-2016 Carbon Cycle As Seen from OCO-2 and the Global in situ Network, Atmospheric Chemistry and Physics Discussions, pp. 1–79, https://doi.org/https://doi.org/10.5194/acp-2019-87, 2019.

D'Arrigo, R., Jacoby, G. C., and Fung, I. Y.: Boreal forests and atmosphere–biosphere exchange of carbon dioxide, Nature, 329, 321–323, https://doi.org/doi:10.1038/329321a0, 1987.

Dee, D. P., Uppala, S. M., Simmons, A. J., Berrisford, P., Poli, P., Kobayashi, S., Andrae, U., Balmaseda, M. A., Balsamo, G., Bauer, P., Bechtold, P., Beljaars, A. C. M., van de Berg, L., Bidlot, J., Bormann, N., Delsol, C., Dragani, R., Fuentes, M., Geer, A. J., Haimberger, L., Healy, S. B., Hersbach, H., Hólm, E. V., Isaksen, L., Kållberg, P., Köhler, M., Matricardi, M., McNally, A. P., Monge-Sanz, B. M., Morcrette, J.-J., Park, B.-K., Peubey, C., de Rosnay, P., Tavolato, C., Thépaut, J.-N., and Vitart, F.: The ERA-Interim reanalysis: configuration and performance of the data assimilation system, Quarterly Journal of the Royal Meteorological Society, 137, 553–597, https://doi.org/https://doi.org/10.1002/qj.828, 2011.

Denning, A. S., Holzer, M., Gurney, K. R., Heimann, M., Law, R. M., Rayner, P. J., Fung, I. Y., Fan, S.-M., Taguchi, S., Friedlingstein, P., Balkanski, Y., Taylor, J., Maiss, M., and Levin, I.: Three-dimensional transport and concentration of $SF_6$. A model intercomparison study (TransCom 2), Tellus, 51B, 266–297, 1999a.

Denning, A. S., Takahashi, T., and Friedlingstein, P.: Can a strong atmospheric CO2 rectifier effect by reconciled with a "reasonable" carbon budget?, Tellus, 51B, 249–253, 1999b.

Dentener, F.: Interannual variability and trend of CH4lifetime as a measure for OH changes in the 1979–1993 time period, Journal of Geophysical Research, 108, https://doi.org/10.1029/2002JD002916, 2003.

Donner, L. J., Horowitz, L. W., Fiore, A. M., Seman, C. J., Blake, D. R., and Blake, N. J.: Transport of radon-222 and methyl iodide by deep convection in the GFDL Global Atmospheric Model AM2, Journal of Geophysical Research, 112, https://doi.org/doi:10.1029/2006JD007548, 2007.

Folkins, I., Bernath, P., Boone, C., Donner, L. J., Eldering, A., Lesins, G., Martin, R. V., Sinnhuber, B.-M., and Walker, K.: Testing convective parameterizations with tropical measurements of HNOsub3/sub , CO, Hsub2/sub O, and Osub3/sub : Implications for the water vapor budget, Journal of Geophysical Research: Atmospheres, 111, https://doi.org/https://doi.org/10.1029/2006JD007325, 2006.

Graven, H. D., Keeling, R. F., Piper, S. C., Patra, P. K., Stephens, B. B., Wofsy, S. C., Welp, L. R., Sweeney, C., Tans, P. P., Kelley, J. J., Daube, B. C., Kort, E. A., Santoni, G. W., and Bent, J. D.: Enhanced Seasonal Exchange of CO2 by Northern Ecosystems Since 1960, Science, 341, 1085–1089, https://doi.org/10.1126/science.1239207, 2013.

Gurney, K. R., Law, R. M., Denning, A. S., Rayner, P. J., Baker, D., Bousquet, P., Bruhwiler, L., Chen, Y.-H., Ciais, P., Fan, S., Fung, I. Y., Gloor, M., Heimann, M., Higuchi, K., John, J., Maki, T., Maksyutov, S., Masarie, K., Peylin, P., Prather, M., Pak, B., Randerson, J., Sarmiento, J. L., Taguchi, S., Takahashi, T., Tans, P., and Yuen, C.-W.: Towards robust regional estimates of $CO_2$ sources and sinks using atmospheric transport models, Nature, 415, 2002.

Heimann, M. and Korner, S.: The Global Atmospheric Tracer Model TM3 Model Description and User's Manual Release 3.8a, Tech. rep., Max-Planck-Gesellschaft, https://www.bgc-jena.mpg.de/bgc-systems/pmwiki2/uploads/Publications/5.pdf, 2003.

Holtslag, A. A. M. and Boville, B. A.: Local Versus Nonlocal Boundary-Layer Diffusion in a Global Climate Model, Journal of Climate, 6, 1825–1842, https://doi.org/10.1175/1520-0442(1993)006<1825:LVNBLD>2.0.CO;2, 1993.

Holtslag, A. A. M. and Moeng, C. H.: Eddy Diffusivity and Countergradient Transport in the Convective Atmospheric Boundary-Layer, Journal of the Atmospheric Sciences, 48, 1690–1698, 1991.

Houweling, S., Dentener, F., and Lelieveld, J.: The impact of nonmethane hydrocarbon compounds on tropospheric photochemistry, Journal of Geophysical Research: Atmospheres, 103, 10 673–10 696, https://doi.org/10.1029/97JD03582, 1998.

Jöckel, P., von Kuhlmann, R., Lawrence, M. G., Steil, B., Brenninkmeijer, C. A. M., Crutzen, P. J., Rasch, P. J., and Eaton, B.: On a fundamental problem in implementing flux-form advection schemes for tracer transport in 3-dimensional general circulation and chemistry transport models, Quarterly Journal of the Royal Meteorological Society, 127, 1035–1052, https://doi.org/https://doi.org/10.1002/qj.49712757318, 2001.

Keeling, C., Bacastow, R., Carter, A., Piper, S., Whorf, T., Heimann, M., Mook, W., and Roeloffzen, H.: A three-dimensional model of atmospheric $CO_2$ transport based on observed winds: 1. Analysis of observational data, 1989a.

Keeling, C., Piper, S., and Heimann, M.: A three-dimensional model of atmospheric $CO_2$ transport based on observed winds: 4. Mean annual gradients and interannual variations, 1989b.

Krol, M., Houweling, S., Bregman, B., van den Broek, M., Segers, A., van Velthoven, P., Peters, W., Dentener, F., and Bergamaschi, P.: The two-way nested global chemistry-transport zoom model TM5: algorithm and applications, Atmospheric Chemistry and Physics, 5, 417–432, https://doi.org/https://doi.org/10.5194/acp-5-417-2005, 2005.

Lee, M. and Weidner, R.: JPL Publication 16-4: Surface Pressure Dependencies in the GEOS-Chem Adjoint System and the Impact of the GEOS-5 Surface Pressure on CO2 Model Forecast, Tech. rep., Jet Propulsion Laboratory California Institute of Technology Pasadena, California, 2016.

Lin, J.-T. and McElroy, M. B.: Impacts of boundary layer mixing on pollutant vertical profiles in the lower troposphere: Implications to satellite remote sensing, Atmospheric Environment, 44, 1726–1739, https://doi.org/https://doi.org/10.1016/J.ATMOSENV.2010.02.009, 2010.

Lin, S.-J. and Rood, R. B.: Multidimensional Flux-Form Semi-Lagrangian Transport Schemes, Monthly Weather Review, 124, 2046–2070, 1996.

Lindqvist, H., O'Dell, C. W., Basu, S., Boesch, H., Chevallier, F., Deutscher, N., Feng, L., Fisher, B., Hase, F., Inoue, M., Kivi, R., Morino, I., Palmer, P. I., Parker, R., Schneider, M., Sussmann, R., and Yoshida, Y.: Does GOSAT capture the true seasonal cycle of carbon dioxide?, Atmospheric Chemistry and Physics, 15, 13 023–13 040, https://doi.org/doi:10.5194/acp-15-13023-2015, 2015.

Liu, J., Wennberg, P. O., Parazoo, N. C., Yin, Y., and Frankenberg, C.: Observational Constraints on the Response of High-Latitude Northern Forests to Warming, AGU Advances, 1, https://doi.org/https://doi.org/10.1029/2020AV000228, 2020.

Lloyd, J. and Farquhar, G. D.: Effects of rising temperatures and [CO 2 ] on the physiology of tropical forest trees, 363, 1811–1817, https://doi.org/10.1098/rstb.2007.0032, 2008.

Malhi, Y., BALDOCCHI, D. D., and JARVIS, P. G.: The carbon balance of tropical, temperate and boreal forests, 22, 715–740, https://doi.org/doi:10.1046/j.1365-3040.1999.00453.x, 1999.

Martin, R. V., Eastham, S. D., Bindle, L., Lundgren, E. W., Clune, T. L., Keller, C. A., Downs, W., Zhang, D., Lucchesi, R. A., Sulprizio, M. P., Yantosca, R. M., Li, Y., Estrada, L., Putman, W. M., Auer, B. M., Trayanov, A. L., Pawson, S., and Jacob, D. J.: Improved Advection, Resolution, Performance, and Community Access in the New Generation (Version 13) of the High Performance GEOS-Chem Global Atmospheric Chemistry Model (GCHP), https://doi.org/https://doi.org/10.5194/gmd-2022-42, 2022.

Molod, A., Takas, L., Suarez, M., Bacmeister, J., Song, I., and Eichman, A.: The GEOS-5 Atmospheric General Circulation Model: Mean Climate and Development from MERRA to Fortuna, Tech. Rep. NASA/TM–2012-104606/Vol 28, National Aeronautics and Space Administration Goddard Space Flight Center, Greenbelt, Maryland, 2012.

Moorthi, S. and Suarez, M. J.: Relaxed Arakawa-Schubert. A Parameterization of Moist Convection for General Circulation Models, Monthly Weather Review, 120, 978–1002, https://doi.org/10.1175/1520-0493(1992)120<0978:RASAPO>2.0.CO;2, 1992.

Naud, C. M., Booth, J. F., and Genio, A. D. D.: Evaluation of ERA-Interim and MERRA Cloudiness in the Southern Ocean, Journal of Climate, 27, 2109–2124, https://doi.org/https://doi.org/10.1175/JCLI-D-13-00432.1, 2014.

Norby, R. J. and Zak, D. R.: Ecological Lessons from Free-Air CO2 Enrichment (FACE) Experiments, 42, 181–203, https://doi.org/https://doi.org/10.1146/annurev-ecolsys-102209-144647, 2011.

Oda, T.: The Open-source Data Inventory for Anthropogenic $CO_2$ , version 2016 (ODIAC2016): a global monthly fossil fuel $CO_2$ gridded emissions data product for tracer transport simulations and surface flux inversions, Earth System Science Data, 10, 87–107, https://doi.org/https://doi.org/10.5194/essd-10-87-2018, 2018.

Orbe, C., Oman, L. D., Strahan, S. E., Waugh, D. W., Pawson, S., Takacs, L. L., and Molod, A. M.: Large-Scale Atmospheric Transport in GEOS Replay Simulations, Journal of Advances in Modeling Earth Systems, 9, 2545–2560, https://doi.org/https://doi.org/10.1002/2017MS001053, 2017.

Peiro, H., Crowell, S., Schuh, A., Baker, D. F., O'Dell, C., Jacobson, A. R., Chevallier, F., Liu, J., Eldering, A., Crisp, D., Deng, F., Weir, B., Basu, S., Johnson, M. S., Philip, S., and Baker, I.: Four years of global carbon cycle observed from OCO-2 version 9 and in situ data, and comparison to OCO-2 v7, https://doi.org/http://doi.org/10.5194/acp-2021-373, 2021.

Penuelas, J., Fernández-Martínez, M., Vallicrosa, H., Maspons, J., Zuccarini, P., Carnicer, J., Sanders, T. G. M., Krüger, I., Obersteiner, M., Janssens, I. A., Ciais, P., and Sardans, J.: Increasing atmospheric CO2 concentrations correlate with declining nutritional status of European forests, 3, https://doi.org/https://doi.org/10.1038/s42003-020-0839-y, 2020.

Peters, W., Krol, M. C., Dlugokencky, E. J., Dentener, F. J., Bergamaschi, P., Dutton, G., von Velthoven, P., Miller, J. B., Bruhwiler, L., and Tans, P. P.: Toward regional-scale modeling using the two-way nested global model TM5: Characterization of transport using $SF_6$, Journal of Geophysical Research-Atmospheres, 109, d19314, 2004.

Peters, W., Jacobson, A. R., Sweeney, C., Andrews, A. E., Conway, T. J., Masarie, K., Miller, J. B., Bruhwiler, L. M. P., Petron, G., Hirsch, A. I., Worthy, D. E. J., van der Werf, G. R., Randerson, J. T., Wennberg, P. O., Krol, M. C., and Tans, P. P.: An atmospheric perspective on North American carbon dioxide exchange: CarbonTracker, Proceedings of the National Academy of Sciences of the United States of America, 104, 18 925–18 930, https://doi.org/10.1072/pnas.07089861074, 2007.

Peylin, P., Law, R. M., Gurney, K. R., Chevallier, F., Jacobson, A. R., Maki, T., Niwa, Y., Patra, P. K., Peters, W., Rayner, P. J., Rödenbeck, C., van der Laan-Luijkx, I. T., and Zhang, X.: Global atmospheric carbon budget: results from an ensemble of atmospheric $CO_2$ inversions, Biogeosciences, 10, 6699–6720, https://doi.org/10.5194/bg-10-6699-2013, 2013.

Posselt, D. J., van den Heever, S., Stephens, G., and Igel, M. R.: Changes in the Interaction between Tropical Convection, Radiation, and the Large-Scale Circulation in a Warming Environment, Journal of Climate, 25, 557–571, https://doi.org/doi:10.1175/2011JCLI4167.1, 2012.

Prather, M. J., Zhu, X., Strahan, S. E., Steenrod, S. D., and Rodriguez, J. M.: Quantifying errors in trace species transport modeling, Proceedings of the National Academy of Sciences, 105, 19 617–19 621, https://doi.org/https://doi.org/10.1073/pnas.0806541106, 2008.

Rienecker, M. M., Suarez, M. J., Gelaro, R., Todling, R., Bacmeister, J., Liu, E., Bosilovich, M. G., Schubert, S. D., Takacs, L., Kim, G.-K., Bloom, S., Chen, J., Collins, D., Conaty, A., da Silva, A., Gu, W., Joiner, J., Koster, R. D., Lucchesi, R., Molod, A., Owens, T., Pawson, S., Pegion, P., Redder, C. R., Reichle, R., Robertson, F. R., Ruddick, A. G., Sienkiewicz, M., and Woollen, J.: MERRA: NASA's Modern-Era Retrospective Analysis for Research and Applications, Journal of Climate, 24, 3624–3648, https://doi.org/https://doi.org/10.1175/JCLI-D-11-00015.1, 2011.

Schimel, D., Stephens, B. B., and Fisher, J. B.: Effect of increasing CO2 on the terrestrial carbon cycle, Proceedings of the National Academy of Sciences of the United States of America, 112, 436–441, https://doi.org/10.1073/pnas.1407302112, 2014.

Schuh, A. E., Jacobson, A. R., Basu, S., Weir, B., Baker, D., Bowman, K., Chevallier, F., Crowell, S., Davis, K. J., Deng, F., Denning, S., Feng, L., Jones, D., Liu, J., and Palmer, P. I.: Quantifying the Impact of Atmospheric Transport Uncertainty on $CO_2$ Surface Flux Estimates, Global Biogeochemical Cycles, 33, 484–500, https://doi.org/https://doi.org/10.1029/2018GB006086, 2019.

Schuh, A. E., Byrne, B., Jacobson, A. R., Crowell, S. M. R., Deng, F., Baker, D. F., Johnson, M. S., Philip, S., and Weir, B.: On the role of atmospheric model transport uncertainty in estimating the Chinese land carbon sink, Nature, 603, E13–E14, https://doi.org/https://doi.org/10.1038/s41586-021-04258-9, 2022.

Stanevich, I.: Variational data assimilation of satellite remote sensing observations for improving methane simulations in chemical transport models, Ph.D. thesis, https://tspace.library.utoronto.ca/handle/1807/89876, 2018.

Stanevich, I., Jones, D. B. A., Strong, K., Keller, M., Henze, D. K., Parker, R. J., Boesch, H., Wunch, D., Notholt, J., Petri, C., Warneke, T., Sussmann, R., Schneider, M., Hase, F., Kivi, R., Deutscher, N. M., Velazco, V. A., Walker, K. A., and Deng, F.: Characterizing model errors in chemical transport modeling of methane: using GOSAT XCH&ampltsub&ampgt4&amplt/sub&ampgt data with weak-constraint four-dimensional variational data assimilation, Atmospheric Chemistry and Physics, 21, 9545–9572, https://doi.org/https://doi.org/10.5194/acp-21-9545-2021, 2021.

Stephens, B. B., Gurney, K. R., Tans, P. P., Sweeney, C., Peters, W., Bruhwiler, L., Ciais, P., Ramonet, M., Bousquet, P., Nakazawa, T., Aoki, S., Machida, T., Inoue, G., Vinnichenko, N., Lloyd, J., Jordan, A., Heimann, M., Shibistova, O., Langenfelds, R. L., Steele, L. P., Francey, R. J., and Denning, A. S.: Weak northern and strong tropical land carbon uptake from vertical profiles of atmospheric $CO_2$, Science, 316, 1732–1735, 2007.

Taszarek, M., Allen, J. T., Marchio, M., and Brooks, H. E.: Global climatology and trends in convective environments from ERA5 and rawinsonde data, npj Climate and Atmospheric Science, 4, https://doi.org/https://doi.org/10.1038/s41612-021-00190-x, 2021.

Tiedtke, M.: A Comprehensive Mass Flux Scheme for Cumulus Parameterization in Large-Scale Models, Monthly Weather Review, 117, 1779–1800, 1989.

Wang, J., Feng, L., Palmer, P. I., Liu, Y., Fang, S., Bösch, H., O'Dell, C. W., Tang, X., Yang, D., Liu, L., and Xia, C.: Large Chinese land carbon sink estimated from atmospheric carbon dioxide data, Nature, 586, 720–723, https://doi.org/https://doi.org/10.1038/s41586-020-2849-9, 2020.

Wu, S., Mickley, L. J., Jacob, D. J., Logan, J. A., Yantosca, R. M., and Rind, D.: Why are there large differences between models in global budgets of tropospheric ozone?, Journal of Geophysical Research, 112, https://doi.org/doi:10.1029/2006JD007801, 2007.

Yu, K., Keller, C. A., Jacob, D. J., Molod, A. M., Eastham, S. D., and Long, M. S.: Errors and improvements in the use of archived meteorological data for chemical transport modeling, Geoscientific Model Development Discussions, pp. 1–22, https://doi.org/https://doi.org/10.5194/gmd-2017-125, 2017.